




Article

Tracking Organomineralization Processes from Living Microbial Mats to Fossil Microbialites

Inès Eymard ^{1,*} , María del Pilar Alvarez ², Andrés Bilmes ³ , Crisogono Vasconcelos ⁴
and Daniel Ariztegui ¹ 

¹ Department of Earth Sciences, University of Geneva, 1205 Geneva, Switzerland; Daniel.Ariztegui@unige.ch

² Instituto Patagónico Para el Estudio de los Ecosistemas Continentales (IPEEC-CONICET), Puerto Madryn, U9120ACD Chubut, Argentina; alvarez@cenpat-conicet.gob.ar

³ En Poste: Instituto Patagónico de Geología y Paleontología (IPGP-CONICET), Puerto Madryn, U9120ACD Chubut, Argentina; abilmes@cenpat-conicet.gob.ar

⁴ Centro de Desenvolvimento Tecnológico (CEDES), Núcleo de Inovação e Tecnologia do Serviço Geológico do Brasil, 22290-180 Rio de Janeiro, Brazil; crisogono.vasconcelos@cprm.gov.br

* Correspondence: ines.eymard@unige.ch

Received: 8 June 2020; Accepted: 2 July 2020; Published: 4 July 2020



Abstract: Geneses of microbialites and, more precisely, lithification of microbial mats have been studied in different settings to improve the recognition of biogenicity in the fossil record. Living microbial mats and fossil microbialites associated with older paleoshorelines have been studied in the continental Maquinchao Basin in southernmost South America. Here, we investigate carbonate crusts from a former pond where active mineralizing microbial mats have been previously studied. Petrographic observations revealed the presence of abundant erect and nonerect microfilaments and molds with diameters varying from 6 to 8 micrometers. Additionally, smaller pores and organic matter (OM) remains have been identified in areas containing less filaments and being dominated by carbonate. A Mg, Al and Si-rich phase has also been identified in the carbonate matrix associated with the dominant micritic calcite. Moreover, mineralized sheaths contain mixed carbonate (calcite) with Mg, Al and Si, where the latter elements are associated with authigenic clays. The presence of mineralized sheaths further attests to biologically induced processes during the uptake of CO₂ by photosynthetic microorganisms. Additionally, the high density of the micritic phase supports the subsequent mineralization by nonphotosynthetic microorganisms and/or physicochemical processes, such as evaporation. Since the micritic filament microstructure of these recent crusts is very similar to that observed in fossil microbialites, they can be used to bridge the gap between living mats and fossil buildups.

Keywords: organomineralization; microbialite; Mg-Si phase; filaments; carbonate; Patagonia

1. Introduction

Microbial mats are composed of diverse microbial communities [1–3]. They have potential for trapping and binding particles and/or to be sites for mineral precipitation, leading to lithification of the mat [3–5]. These accreted and lithified microbial mats form organosedimentary deposits, also referred to as microbialites [6]. Microbialites and, more specifically, stromatolites are widespread throughout geological time, from the Early and Late Archean [7–9] until now [10–13]. They have been identified occurring in various settings, such as marine, lacustrine and fluvial (e.g., tufas), as well as in extreme hypersaline environments, high altitude lakes and exceptionally hot water pools [14–19]. Their distribution, mineralogy and geochemistry can provide valuable information for paleoenvironmental reconstructions [20–23].

Mineralization processes in microbial mats, also referred to as organomineralizations, are complex because they involve the interplay between intrinsic (microbial assemblages, microbial metabolism and their resulting processes) and extrinsic factors (physicochemical processes) [24]. However, in many cases, the term organomineralization may have different significance related to its long and controversial history (e.g., [25–28]). Understanding extrinsic versus intrinsic interactions is critical for geobiological investigations and for sedimentology in general. In the geological record, it is often unclear whether the observed structures are of biogenic or nonbiologic origin [29], making it difficult to classify them as microbialites. Conversely, the study of modern “living” microbial mats allows for a more precise analysis of biogenic structures that can be used as analogs for the fossil record. Early investigations, which focused on mineralization processes in microbial mats, have already highlighted the importance of cyanobacteria (photosynthesis) and extracellular polymeric substance (EPS) degradation in triggering carbonate precipitation [24]. Further research has also shown that nonphotosynthetic microorganisms, such as sulfate-reducing bacteria (SRB), as well as heterotrophic bacteria, play a significant role in carbonate precipitation processes [30]. Finally, environmentally controlled factors, such as $p\text{CO}_2$, the presence of springs and/or the mixing of chemically different waters, as well as evaporation, can also promote carbonate precipitation [31,32]. Applying these modern observations to studies of ancient examples has resulted in the inference of different mineralization processes in the formation of fossil microbialites.

Understanding the complex and subtle balance between extrinsic and intrinsic parameters in microbialite formation is critical to define mineralization processes in both fossil microbialites and their modern analogs. Nevertheless, the presence of living microbial mats does not always imply mineralization, as both lithifying and nonlithifying examples exist. While some microbial communities promote carbonate precipitation, others can prevent it [24,30,33]. As there are a wide variety of microbialites, it is fundamental to identify which settings can promote lithification, which conditions support the conservation of microbialites and which microbial traces are preserved. The recognition of microbial traces is fundamental to improving the assessment of evidence for biogenicity in the fossil record.

The Maquinchao Basin in Northwestern Patagonia, Argentina, provides a unique opportunity to explore the role of different aspects and stages of mineralization (Figure 1A). The basin contains Pleistocene microbialites associated with a former large lake [34], along with living mats precipitating carbonates [35]. The Maquinchao Basin is a closed endoreic basin located in the Argentinian province of Rio Negro. It is composed nowadays of two main lakes, connected by the ephemeral Maquinchao River, partially sustained by groundwater. Fossil microbialites attest to a former higher water level in the basin [34,36]. Living and mineralizing mats were observed in 2011 in several ponds of the Maquinchao River [35]. These were described as globular mats containing low-Mg calcite minerals with a higher mineral content in their lower part. Organomineralization, *sensu* Dupraz et al. [24], in the mats has been associated with photosynthetic activity in the upper part of the mat and heterotrophic microorganisms in the lower part of the mat. From 2015 onward, several areas of the Maquinchao River containing living mats have dried out. This environmental event provides us with a unique opportunity to study the sequences of changes affecting microbial mats that have recently become desiccated. In this contribution, we track the sequence of changes affecting the living microbial mats through to their mineralization. Additionally, we provide a valuable dataset to better understand both mineralization and/or organomineralization *sensu* Dupraz et al. [24] and preservation processes affecting mat alteration through time. In this study, we have identified the changes occurring in the progression from “living” to “dead” mats during a five-year interval and compared their observed similarities and differences with fossil buildups found in the same region. This interpreted formation sequence may be further applicable to other fossil microbialites outcropping in similar lacustrine environments.

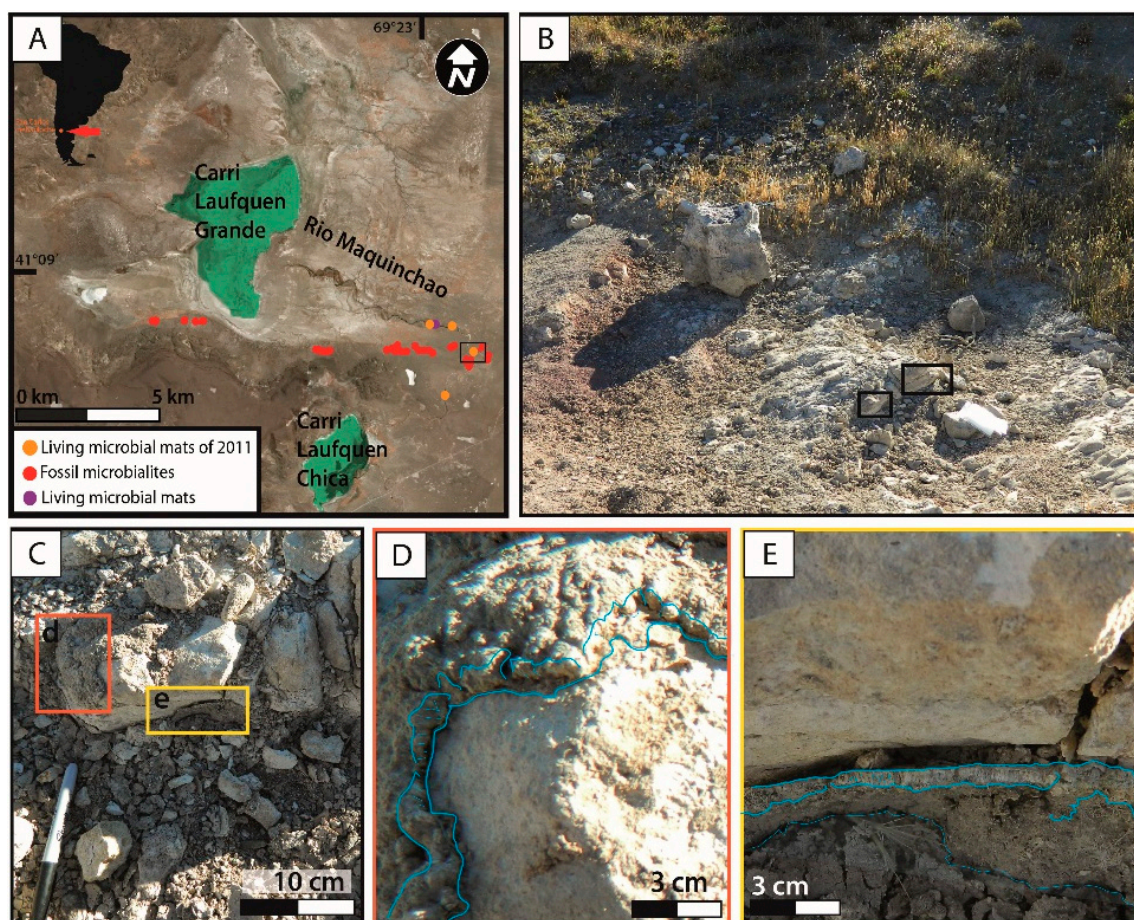


Figure 1. Sampling area. (A) Map of Maquinchao Basin with the location of living microbial mats in 2011 and 2016, fossil microbialites and sampling location of modern microbial crusts (black square). (B) Enlargement of black square in (A). Black rectangles enclose crusts on hard substrate. (C) Enlargement of area shown in (B), highlighting the crusts on the top and lateral side of the hard substrate. (D) Enlargement of the orange rectangle in (C), showing the pustular-like crust on the hard substrate. (E) Enlargement of the yellow rectangle in (C), showing the smooth crust probably attached to the rock substrate in the Figure 1C.

2. Materials and Methods

Several field campaigns were carried out in the Maquinchao Basin during the last ten years. Carbonate crusts were sampled in January 2017 from a former pond of the Maquinchao River, which contained living mineralizing mats in 2011 [35] and, subsequently, dried out, remaining desiccated since at least the Austral summer 2015 (Figure 1). Selected pieces of crusts were impregnated with a bicomponent resin epoxy (Araldit® XW396/XW 397) to prepare standard thin sections. Microscopic observations were performed before further inspection via cathodoluminescence, μ -XRF and SEM imaging at the University of Geneva (Geneva, Switzerland). Cathodoluminescence analyses were conducted using an optical cold cathodoluminescence system (model Cathodyne from NewTec Scientific) mounted on an Olympus BX41 petrographical microscope (Olympus, Tokyo, Japan). The beam conditions were 18 kV at 120–200 μ A, with an unfocused beam of approximately 1 cm. The observation chamber had a residual pressure of approximately 50 mTorr. Qualitative maps of elemental composition were obtained at a micrometer resolution using an EAGLE III μ -XRF scanner (Edax Inc., Mahwah, NJ, USA). Analyses were conducted under vacuum conditions with a 50- μ m-diameter beam. Selected slabs were measured for Al, Ba, S, Ca, Mn, Fe and Ti. Data are expressed as elemental intensities in counts per second (cps). Selected thin sections were carbon coated

for SEM inspection and energy-dispersive microscopy (EDS) analyses using a JEOL 7001 PA scanning electronic microscopy, equipped with an energy-dispersive X-ray analyzer EDS JED2300. Small pieces without impregnation but gold coating have been further used for SEM and EDS observations and analyses. In addition, X-ray diffraction (XRD) analyses and CT scanning have been carried out on selected pieces of the crust. Mineralogical analyses were performed at the University of Geneva. XRD facilities using a Philips X'pert, equipped with a PW3710 MPD diffractometer and a PW3020 vertical goniometer. A total of six thin sections were successfully prepared. Three of the thin sections comprised two sample pieces each, and the other three thin sections contained samples mounted with their basalt substrates. Three thin sections were studied using cathodoluminescence, μ -XRF and SEM. Additionally, several pieces of carbonate crust of less than 2 mm were mounted on stubs for SEM observation.

3. Results

A field campaign was carried out in 2011, and living microbial mats were identified and sampled for the first time in several ponds of the Maquinchao Riverbed [35]. Successive field campaigns (i.e., in 2015–2018) revealed that the ponds containing microbial mats had dried out completely (Figure 1A,B), and the water level of Carri Laufquen Grande had undergone fluctuations [36]. However, several mineralized microbial mats were preserved on hard substrates mostly of basaltic composition. In some cases, crusts could be observed directly on top of basalts, on their sides or very close to them (Figure 1C). They were a few millimeters thick (2–4 mm), displaying either a pustular or a smoother surficial texture (Figure 1D,E). The lateral extension of the crusts on the hard substrate was relatively limited, because the crusts did not entirely cover the basalts and were not always preserved on all the outcropping basalts.

At first glance, these crusts appear to be homogenous. However, with a closer look at the thin sections under the microscope, two types can be differentiated: a dense crust (Figure 2A) and a porous crust (Figure 2B). The dense crust displays lamination and fan-like structures (Figure 2A,C). A color difference from brownish to yellow-green can be observed in the dense crust (Figure 2A,C,D). When present, micrite is associated with the more brownish areas (Figure 2D,E). The more yellowish color is associated with organic matter (OM) present in the erect elongated structures of filamentous microorganisms (Figure 2D,E). They have less than 10- μ m widths and are several tens of micrometers in length. However, the high density of erect elongated structures makes it difficult to precisely determine their lengths. In addition, diatoms and other microorganism can be observed in the thin sections (Figure 2D,E). Finally, the lowermost part of the fan structure presents a high concentration of rounded pores of 6- μ m to 9- μ m diameters in a micritic matrix (Figure 2G). Those pores become elongated and greenish-yellow in color when located in the uppermost part of the samples.

Porous crusts have similar features as the dense crusts but are less compact. Brownish micrite, as well as elongated structures, are scarcer in the thin section (Figure 2F), leading to a highly porous structure. Elongated structures have a similar width, ranging from 6 μ m to 12 μ m and from 90 μ m to 130 μ m in length. The yellowish color is also less present than in the dense crusts (Figure 2B,F) with associated micrite and microsparite. Although a lower number of rounded pores are observed, they have a similar diameter, ranging from 6 μ m to 10 μ m. Finally, the uppermost sections of the crusts display dense micrite and an obvious lack of the elongated filamentous structures in comparison to the rest of the sample (Figure 2D,F). Patches of well-preserved diatoms are found in the crusts (Figure 2H), but they are more abundant in the porous crust compared to the dense crust.

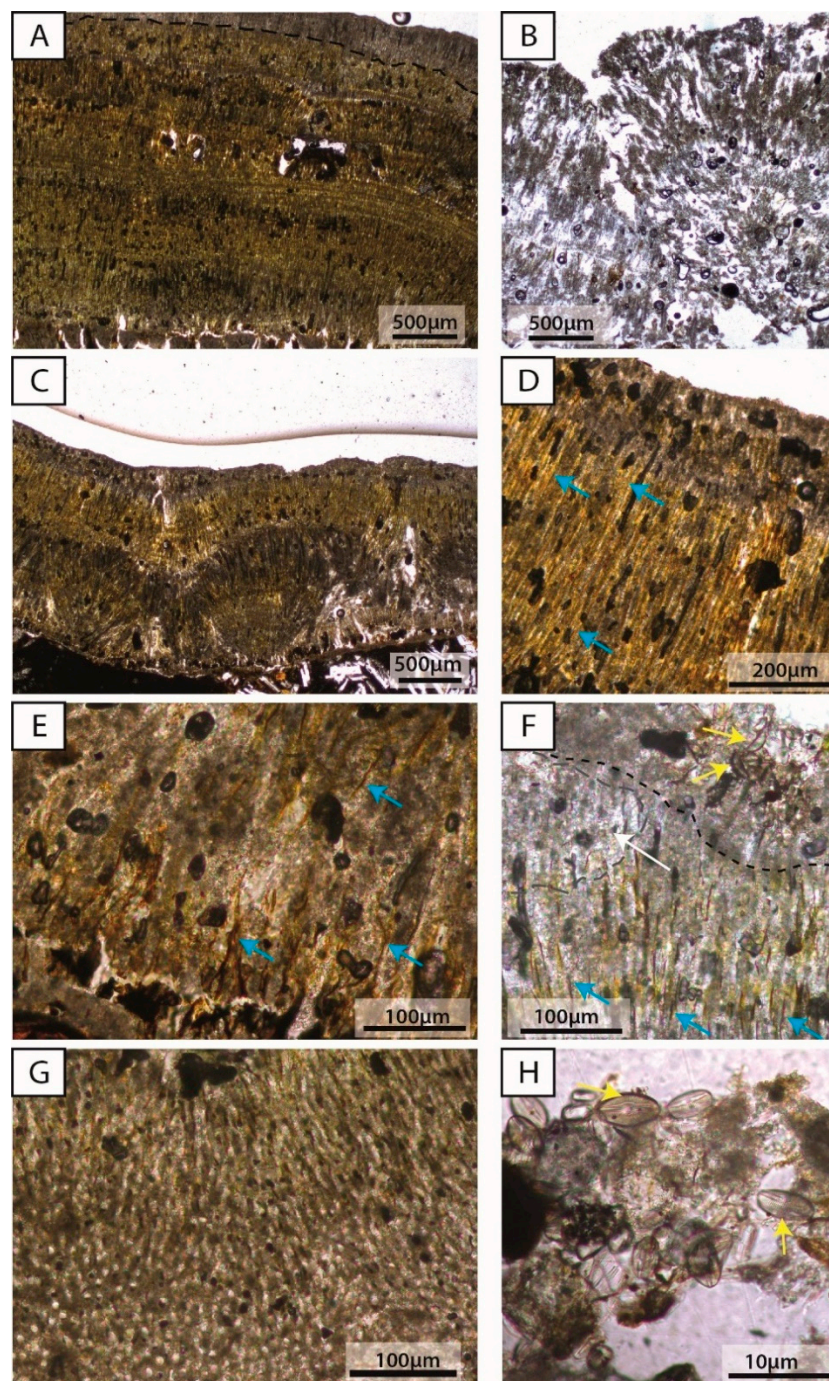


Figure 2. Photomicrographs under the transmitted light of the thin sections of the dried crust samples (Figure 1). (A) Dense crust with slightly visible plane parallel laminations. (B) Porous crust. (C) Dense crust and fan-shaped structure visible in the lower portion. (D) Enlargement of the upper part of the dense crust. Blue arrows show filaments. (E) Enlargement of the lower section of the dense crust with visible micrite. Blue arrows show filaments. (F) Enlargement of the porous crust. Diatoms are visible in the upper part (yellow arrows). White arrow shows the microsparite area. The micrite is homogenously distributed in the rest of the photograph; microorganisms (yellow arrows) and elongated filamentous structures (blue arrows) can be observed. (G) Enlargement of the lowest part of the fan-like structures of the dense crust. Homogenous, rounded pores are visible in the micrite observed in the lower part, while the upper part contains more elongated filaments. (H) Diatoms (yellow arrows) and other microorganism contained in the upper part of the porous crusts.

Under cathodoluminescence, both crusts show different intensities, from orange to dull luminescence and close to nonluminescent (Figure 3). The orange luminescence, typical of calcite, shows variable intensities in the samples (Figure 3). Changes in the luminescence intensity are more visible in the dense crusts (Figure 3A,C,E) compared to the porous crusts (Figure 3B,D). Luminescence appears to highlight structures such as fans in the dense crusts and nodular mineralized structures in the lower parts of the mats (Figure 3A). In some cases, changes in the luminescence intensity reveal clear lamination not visible under normal light (Figure 3E), which enhances the visualization of differences in the growth structures (Figure 3B,F). Furthermore, the filament-like structures and pores are sharper under cathodoluminescence, because they are not luminescent compared to the mineralized carbonate crust (Figure 3F).

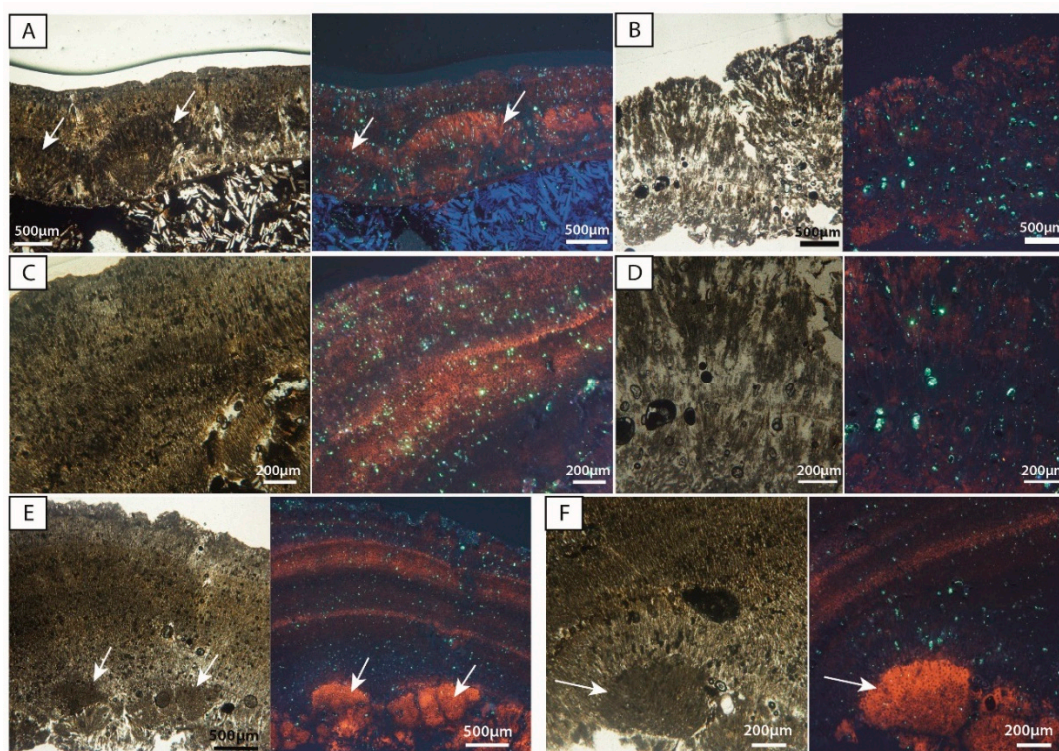


Figure 3. Photomicrographs showing paired thin sections under plane polarized light and associated cathodoluminescence. (A) Dense crust on basalt substrate. Fan-like shapes (arrows) stand out under cathodoluminescence. (B) Porous crust. (C) At higher magnification of the dense crust, laminae are visible under cathodoluminescence. (D) At higher magnification of the porous crust, slight changes in luminescence under cathodoluminescence are observed. (E) The dense crust showing that clear laminated structures of different luminescence are visible under cathodoluminescence. White arrows show highly luminescent concretions. (F) Higher magnification of the rounded structure shown in (E), indicated by white arrows. The rounded structure is more luminescent than the surrounding matrix.

Elemental mapping using μ -XRF confirmed the cathodoluminescence observations, indicating a high calcite content (Figure 4). The basaltic substrate is characterized by high concentrations of Al and Fe, as well as high concentrations of Ba and Ti (not displayed) (Figure 4B,C). These same elements are also identified in clasts/grains observed trapped within the (former) microbial mat, whereas K and Mn can also be observed in the basalt substrate. As expected, the crusts present a strong and dominant Ca signal (Figure 4A–C), as well as a S signal that is observed in the three studied samples. The most external edge of the crust that is in direct contact with the environment contains a very thin layer containing Al and Fe, as well as Ba and Ti (not displayed) (Figure 4A). These elements may be associated with detrital particles, the presence of which are most probably related to the trapping of weathered and eroded particles of basalts in the original microbial mat.

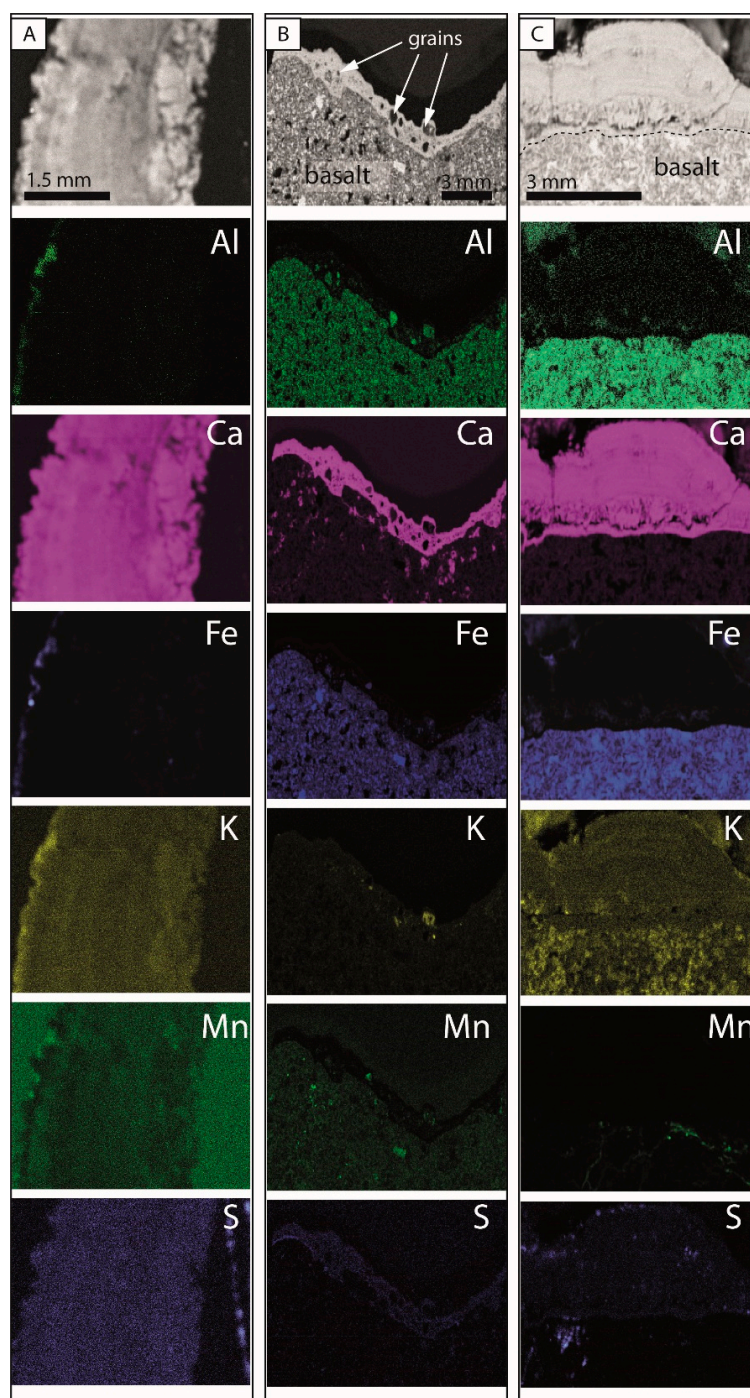


Figure 4. Microfluorescence mapping of elemental Al, Ca, Fe, K, Mn and S. (A) Dense crust. (B) Dense crust associated with extracrust and basalt substrate. (C) Dense crust on basalt substrate.

SEM observations (Figures 5 and 6) indicate differences in microstructures between the upper surface and the lower part of the crusts in whole pieces (Figure 5) and thin section (Figure 6). In whole crust pieces (Figure 5A), the upper part of the crust presents scarce rounded pores (Figure 5B) and diatoms (Figure 5C). Minerals are present as irregular small particles. The rest of the crust presents a dense assemblage of pores of tubular shapes that appear to be molds of filaments (Figure 5D,E). Although sometimes difficult to assess, the diameters of the pores range between 6 μm and 8 μm . Filament structures are observed in some of the pores (Figure 5B,D,E). Certain filaments seem to be mineralized (Figure 5F), whereas others still look like more organic material (Figure 5G).

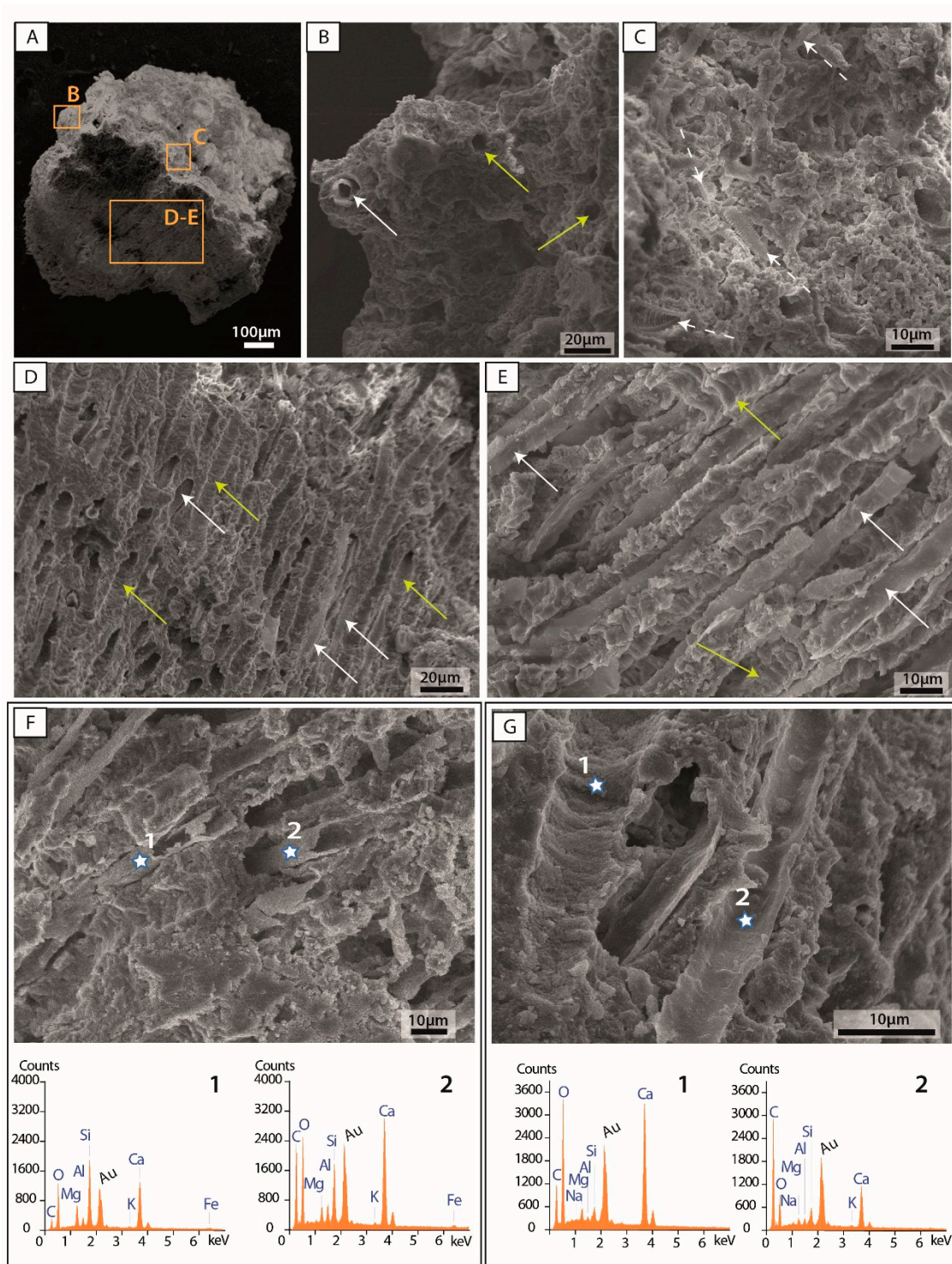


Figure 5. SEM photomicrographs and energy-dispersive microscopy (EDS) analyses of pieces of dried crusts. (A) Piece of crust. Rectangles highlight areas shown in the following SEM photomicrographs. (B) At higher magnification, rectangle B shows rounded pores (yellow arrows) and a rounded pore with a preserved filament sheath (white arrow). (C) At higher magnification, rectangle C reveals the presence of diatoms (dashed white arrows). (D) Under higher magnification of rectangle D,E, filament remains are indicated by white arrows, whereas yellow arrows point to filaments molds. (E) Under higher magnification of rectangle D,E, organic filaments are indicated by white arrows, whereas yellow arrows point to mineralization. (F) SEM photomicrograph of rectangle D,E showing the position of two EDS analytical measurements on the mineralized filament-like structures. (G) Rectangle D,E showing the position of associated EDS analytical measurements on the filament molds (1) and organic matter (OM) filament remains (2).

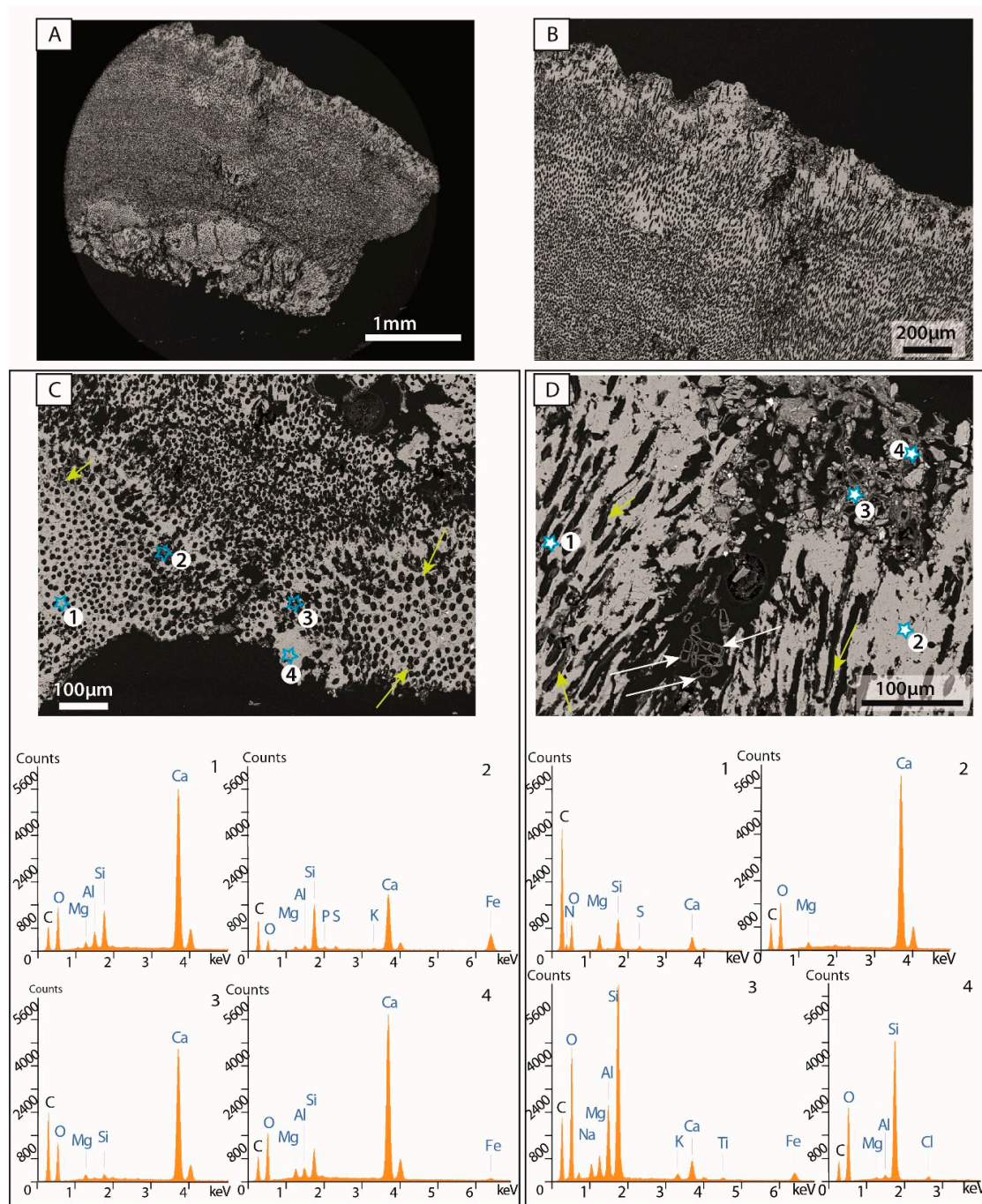


Figure 6. SEM photomicrographs and EDS analyses on thin sections of dried crusts. (A) SEM photomicrograph of the dense crust thin section. (B) Higher magnification of the upper part of the dried crust (A), with distinctly rounded and elongated microstructures. (C) SEM photomicrograph showing the positions of EDS analytical measurements with different areas of the mineralized crust (1–4). Yellow arrows point to filament remains in the rounded pores. (D) SEM photomicrograph showing the position of EDS analytical measurements associated with different elements: (1) filament remains, (2) carbonate crust, (3) detrital clasts and (4) detrital clasts. Yellow arrows indicate filament remains in the tubular pores, while white arrows point to diatoms.

Since carbonate is the main mineral of the crust, the Ca signal is always present when doing EDS analyses on both the mineralized part and the filaments (Figure 5F,G). Nevertheless, the Ca readings are stronger when analyzing dense crust sections than in the filaments. Conversely, the carbon signal

is clearly stronger on the filament remains (Figure 5F,G). Interestingly, Mg, Al and Si are detected by EDS (Figure 5F,G), and their signal is stronger for analytical points on mineralized filament structures (Figure 5F) compared to analytical points on filament molds (Figure 5G).

SEM observations of thin sections (Figure 6) show clear variations in porosity (Figure 6A,B). The microporosity decreases with the increasing amount of dense carbonate microfabrics. Elongated tubular structures vary from 7 to 8- μm -wide, increasing to 8–10 μm when not very well-preserved. Rounded structures have a diameter of 7 to 8 μm when they are well-defined and preserved. Additionally, smaller rounded-like structures/pores can be identified in the carbonate matrix, with a diameter of 1 to 2 μm . Finally, the upper part of the crust shows a clear lack of tubular pores compared to the lower part of the same crust. Patches of detrital remains, as well as diatoms, are found mostly in the uppermost part of the crust (Figure 6B,D). Ca is clearly the main component of the mineralized crust (Figure 6C,D). Nevertheless, in most EDS analyses of the mineralized part, Mg, Al and Si are also detected (Figure 6C). Differences in signals can be identified depending on the location of the analytical point in the sample. Patches of detrital/external materials include Mg, Al and a high signal for Si. Additionally, Fe, Ti and Cl are detected, whereas Ca is very low (Figure 6D). On the other hand, areas of dense crusts without rounded or tubular pores have a strong signal for Ca with a very low signal for Mg and, in some cases, a low signal for Si (Figure 6C,D). Areas with either abundant rounded or tubular pores have a strong EDS signal strong in Ca and the substantial presence of Mg, Al and Si. Filament remains are often present within tubular and rounded pores (Figure 6C,D). EDS analyses of these samples with filament remains show a distinct carbon signal associated with N, Mg and Si. Small amounts of S can be also detected, whereas the Ca signal is lower than in the crust (Figure 6D).

Finally, very small rounded structures of 1–2 μm diameters are observed in SEM photomicrographs of the thin section, as well as bacilli-like shapes (Figure 7A,B). In porous samples, large filament structures encase round to semi-elongated pores (Figure 7B,C), suggesting that the development of significant porosity occurs after lithification of the crusts. XRD analyses and EDS analytical measurements on the dried crusts indicate the presence of low-Mg calcite as the dominant mineral.

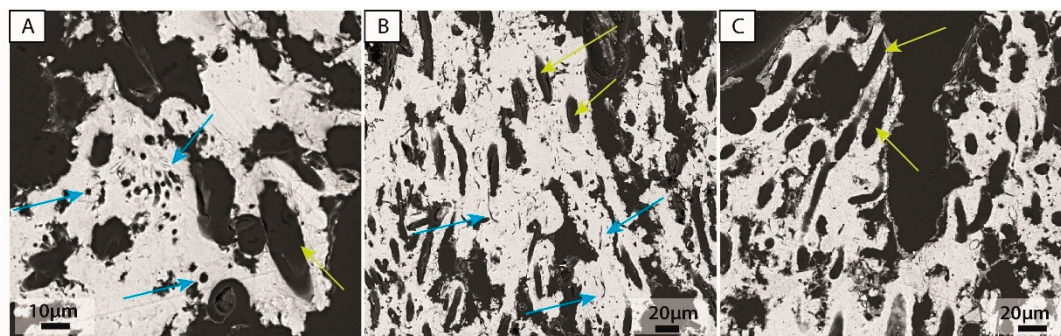


Figure 7. SEM photomicrographs of the porous dried crust thin section. (A) Photomicrograph showing 1 to 2- μm -diameter rounded microstructures and other small elongated microstructures. Blue arrows indicate the small microstructures, whereas the yellow arrow points to the filament pores. (B) Photomicrograph showing filament remains and smaller microstructures. Blue arrows indicate the smaller microstructures, whereas yellow arrows point to the filament remains. (C) Photograph showing the filament remains associated with large pores. Yellow arrows indicate the pores of filament remains.

4. Discussion

4.1. Study of Living Microorganisms Providing Hints to Their Identification in the Fossil Record

Microbial mats are often described as complex assemblages of microorganisms mostly organized in discrete layers [3]. Their less complex form is called a biofilm [3]. From top to bottom, a typical complex layered sequence contains the following microorganisms: oxygenic photosynthesizers, aerobic heterotrophs, anoxygenic phototrophs and anaerobic heterotrophs [24,37]. Although mats

comprise organic/biogenic matter, once they are lithified and the original organic matter (OM) decays, the identification of former microorganisms becomes difficult, and, thus, the assessment of the former biogenicity of the sediments is problematic [29].

The lithified crusts in the Maquinchao Basin are most likely associated with microorganisms based on the rounded and tubular microstructures observed within the samples. In the uppermost part of the crusts, the porosity produced by the rounded and tubular microstructures is less than in the rest of the crust (Figure 6). Since the porosity is rarely open to the upper surface, it is highly unlikely that the pore spaces are due to boring microorganisms [38]. Thus, these crusts are most probably the result of an organomineralization process (*sensu* Dupraz et al. [24]).

Four different microorganisms or their traces have been observed in the studied modern dry crusts. Diatoms on the top of samples, rounded microstructures of 7–8- μm diameters, tubular pores with a width between 7 and 9 μm and very small rounded pores of 1–2- μm diameters combine to create the observed porosity (Figure 7). SEM observations in both longitudinal and perpendicular profiles (Figure 5) suggest that the large rounded and tubular microstructures have the same origin. Due to the prominent presence of these two microstructures in the samples, it is proposed that they are the result of the dominant microorganisms living in the crusts during their formation. Additionally, the observed greenish-yellowish OM remains in thin sections appear to be associated with the tubular pores and filamentous remains. Roche et al. [17] and Payandi-Rolland et al. [39] have described the presence of filament molds of similar diameters in microbialites and have associated them with filamentous cyanobacteria. The association of greenish-yellowish OM remains and tubular pores suggests that a photosynthetic microorganism is most likely to be responsible for the tubular porosity. Unbranched filamentous cyanobacteria, such as *Microcoleus*, *Phormidium* and *Oscillatoria*, have been previously described in active microbialites producing both molds and filaments in modern environments similar to the Maquinchao Basin [39]. Freytet and Verrecchia [40] have described other filamentous benthic cyanobacteria from freshwater environments that can occupy both erect or horizontal positions. The orientation of the filaments seems to be dependent on the energy of the environment, with erect filaments being preferentially observed in low-to-medium energy environments [41,42]. It is clear that, in the Maquinchao Basin carbonate crusts, the OM remains and associated tubular structures are products of filamentous cyanobacteria. However, neither the OM remains nor the observed structures are distinctive enough for a precise taxonomic identification. In addition to the large tubular pores, smaller microstructures of 1–2- μm diameters are present in the dried carbonate crusts. Pacton et al. [35] have identified coccoid and filamentous cyanobacteria with similar diameters in living microbial mats associated with their study of the fresh-water stromatolites (See Figures 8a,d and 10 from [35]). They also reported the presence of sulfate-reducing bacteria (SRB) (See Figure 8f). Hence, the observed structures in the mineralized crusts of the Maquinchao Basin, which display diameters between 1 and 2 μm , are most probably the remains of the living communities, as described by Pacton et al. [35]. Additionally, Pacton et al. [35] reported that diatoms were present in the upper surface of their living microbial mats, similar to the diatoms reported for the dried crusts in this study.

In 2011, filamentous cyanobacteria were extensively observed in the living microbial mats from the Maquinchao Basin. However, it is not clear whether the large filamentous phototrophs/cyanobacteria from the dried crusts are the same as the filamentous cyanobacteria observed in the living mats in 2011, because the modern filaments were thinner (Figures 8 and 10 Pacton et al. [35]). This difference in size might be related to changes in the population through time (from 2011 to 2015) and/or the preferential preservation of certain microorganisms over others when mineralization occurs. Alternatively, the differences in microbial communities between the 2011 living mats and the post-2015 mineralized crusts might be linked to a change in community structures related to the transport time and storage conditions of the living samples (plastic and aluminum foils for more than 48 h hours due to car/bus/plane transportation) between the sampling and observations in 2011.

Microfabrics of the Pleistocene microbialites of the Maquinchao Basin have been investigated [34], thus allowing to make parallels between Pleistocene fossils and modern crusts. Although less abundant,

similar elongated pores to those observed in the modern crusts averaging 8- μm diameters are also observed in the Pleistocene samples of the Maquinchao Basin [34]. Additionally, the cathodoluminescence inspection of these Pleistocene buildups has revealed micrometric (1–2- μm)-sized microstructures of rounded or more irregular shapes [34]. Thus, these microstructures observed in the fossil buildups could be the Pleistocene equivalent of the 1–2- μm diameter microstructures observed in the modern dried crusts. This suggests that the large Pleistocene microbialites might contain similar types of large filamentous cyanobacteria and possibly other smaller microorganisms, as observed in the modern dried crusts. It further appears that large filamentous cyanobacteria can play a major role in both fossil and dried crust formations. Thus, the similarities between micritic microfabric in the fossil buildups, lithified crusts and modern mats permit a further comparison providing new data to better understand their overall formation processes.

4.2. Microtextures and Prevailing Mineralogy

Microbialites, in general, and stromatolites and travertine, in particular, display repetitive patterns shown as changes in microtextures. Often, in the absence of diagenesis, they exhibit an alternation of micrite and sparite laminae, which usually are interpreted as biotic (micrite) and abiotic (sparite) markers [31,42,43]. In sparite-laminated travertine/tufa, the successive laminae permit the observation of the growing surface, providing a good indication of the growth direction. Furthermore, several authors have associated the presence of sparite with the lack of microorganisms [31,42–44]. Conversely, micrite is mostly observed in environments containing abundant microorganisms [31,41].

Calcite is the prevailing mineral in the Maquinchao Basin crusts, as demonstrated by different analytical techniques. The dominant Ca signal in $\mu\text{-XRF}$ and EDS analyses, along with the orange color under cathodoluminescence, are typical indicators for calcite [45]. These observations have been further confirmed by XRD analyses. The EDS analyses of the calcite matrix in thin sections yields Mg/Ca ratios of 0.02 to 0.03, indicating the presence of low-Mg calcite. Low-Mg calcite has been identified as the dominant mineral phase in the Pleistocene microbialites [34], dried crusts and mineralizing living mats [35] of the Maquinchao Basin, suggesting low-Mg calcite is a primary origin rather than resulting of the replacement of a less-stable carbonate phase. Observations under normal microscopy and SEM of both dense and porous crusts indicate that calcite is mostly present as a micrite. Microsparite was observed in certain areas of the porous crusts. There is a clear absence of lamination at the microscopic level.

The absence of alternating micrite and microsparite/sparite laminae in the dried crusts suggests homogeneous environmental conditions in terms of the energy and balance between intrinsic and extrinsic parameters. Sparite formation is often associated with high-energy environments (dams, falls and wave impacts) and winter (cold) periods [31,41,43], because, under these conditions, microbial communities are less likely to develop [41]. It has been shown that the lack of microorganisms associated with high- $p\text{CO}_2$ and the saturation index promote abiotic carbonate precipitation, such as sparite [31]. On the other hand, micrite precipitation may be the result of biotic processes (metabolic activity) or abiotic processes (evaporation and degassing) in a low-energy environment and associated with the presence of microbial communities.

The Pleistocene fossil microbialite buildups of the Maquinchao Basin display two main microfabrics: (1) micritic with filaments and (2) laminated microspar/sparite and micrite [34]. The microfabric (1) show distinctive similarities with the dried crusts, including the mineralogy (low-Mg calcite), the dense micrite and the tubular pores, although the latter are less abundant [34]. Pacton et al. [35] reported the presence of low-Mg calcite concretions in the lower part of the living microbial mats sampled in 2011 and a lower amount of low-Mg calcite crystals in the green/photosynthetic part of the mat.

The dried crusts are homogenous in terms of microstructures. Nevertheless, alternate changes in the degree of luminescence display a lamination pattern not visible under normal microscopy. There is no apparent relationship between the changes in luminescence and the density of pores and/or micrite. Furthermore, no clear changes in microtextures (alternance between micrite and microspar) are visible, implying that physiochemical parameters are most probably responsible for the alternating

strong and dull-to-none luminescence. According to Machel [46], changes in luminescence are related to the presence and/or absence of activator and inhibitor elements (Mn being an activator and Fe being an inhibitor, plus Rare Earth Elements, REE, for calcite). In fact, even if the concentrations are very low, some areas appear to be more enriched in Fe (Figures 5 and 6), thus resulting in low-to-nonluminescent zones. As the riverbed in the Maquinchao Basin is linked to both groundwater and meteoric water inputs [35], the lamination displayed under cathodoluminescence might be related to alternating changes in the main source of the water. These different sources contain distinctive chemical concentrations in the inhibitor/activator (more or less rainfall) or simply a variable elemental concentration in the water, either as a result of an external source (e.g., volcanic ashes) or the increasing evaporation in the pond.

4.3. Calcite Precipitation in Crusts, Induced versus Influenced Organomineralization

Organomineralization can be either biologically induced or biologically influenced [35]. Intrinsic parameters, such as microbial metabolism, are critical in biologically induced mineralization [35], whereas extrinsic parameters and, therefore, environmentally driven conditions, such as degassing, evaporation and saturation in different elements, among others, are vital in biologically influenced mineralization [35]. Several distinctive areas can be identified: the lithified crusts of the Maquinchao Basin, based on the differences in microorganism remains and the matrix microstructure. Crusts are characterized by the dominant presence of dense, tubular pores that are remnants of former filamentous microorganisms in a micritic matrix. The lower parts of the crusts comprise nodular shapes, and the upper parts of the mats are depleted in filamentous pores and remains, yielding dense micrites compared to the rest of the crust. Thus, suggesting that, even in these millimeter-thick dried crusts, various different processes could have led to calcite precipitation.

The preservation of the tubular pore structures in the Maquinchao Basin dried crusts is ideal for precisely determining the orientation and location of individual former filaments. Merz-Preiss [22] and Merz-Preiss and Riding [47] have focused on microbial filament encrustation in active modern systems, where encrustation mechanisms are associated with mineral formation on the filament sheaths. This process leads to the formation of a tube mold after the decay of the OM. Merz-Preiss and Riding [47] have described encrustation phenomena observed with filaments found in a fluvial system with abiotic CO₂ uptake under high dissolved inorganic carbon (DIC) conditions and the saturation index (SI). However, the encrustation of filaments is not only restricted to fluvial settings, having been described in systems where evaporation has a substantial impact [48,49]. Encrustation is driven by extrinsic parameters (CO₂ degassing and evaporation) and, therefore, is a biologically influenced mineralization process. Encrustation seems to be the preferential process in dried crust mineralization. The Maquinchao Basin crusts, however, contain not only molds of filaments (suggesting the encrustation of filamentous cyanobacteria) but, also, mineralized filament sheaths representing the different stages of preservation (Figure 5). Although sheaths are mineralized, the mineralization of the inner part of a filament itself is very rare in the observed crusts. Merz-Preiss [22], Gradziński [41], Merz-Preiss and Riding [47] and Wacey et al. [50] have reported the mineralization of cyanobacteria filament sheaths in microbial mats. Merz-Preiss and Riding [47] have described the calcification of the sheath in low-energy environments, representing low DIC and SI_{calcite} values between 0.2 and 0.8. The associated mechanism of CaCO₃ precipitation was inferred to be biotic activity and defined as an impregnation process. The impregnation of cyanobacteria sheaths in that context resulted from the uptake of CO₂ by the photosynthetic activity of cyanobacteria. Since mineralized sheaths are not observed uniformly in the Maquinchao Basin crusts, it can be inferred that both encrustation and impregnation occur in the crusts. However, the biologically induced process of impregnation is restricted to areas of molds associated with preserved/mineralized filaments sheaths. Most impregnation/encrustation studies have been conducted in simple ecosystems composed of cyanobacteria and diatoms. Thus, our understanding of impregnation/encrustation processes in more complex microbial mat ecosystems comprising diversified

microorganisms is quite limited [24]. Therefore, the potential impact of other metabolism in the mineralization process cannot be ruled out [24].

The Maquinchao Basin dried crusts are characterized by extensive filamentous cyanobacteria molds and preserved sheaths. However, the presence of other microorganisms and their impacts on the mineralization process when the living mat was still active cannot be discarded. Traces of other microorganisms of smaller sizes have been revealed in the crusts (Figure 6). Pacton et al. [35] have previously described the complex assemblages of microbial communities while pointing out the presence of SRBs, among others. Moreover, large low-Mg calcite concretions have been interpreted as having been precipitated by the actions of heterotrophic metabolism and OM degradation [35]. In the dried crusts, calcite concretions are observed in the lower parts of the crusts (Figure 3E). The presence of concretions in similar locations in both dried crusts and their 2011 living counterparts suggests similar processes of formation for the crust nodules/concretions. Heterotrophic metabolic reactions, such as a sulfate reduction and release of Ca^{2+} by degradation of the OM (EPS and/or sheaths and cells), would increase the alkalinity and provide the elements necessary for carbonate precipitation [24,30,37,51,52], leading to the formation of the concretions observed in the lower part of the dried crusts.

The uppermost part of the dried crust does not display tubular pores or filament remains, although carbonate precipitation still occurs, producing a dense texture. In its living analog (living mats from 2011), low-Mg calcite precipitation occur preferentially in the lower part of the mat associated with an increasing alkalinity resulting from the metabolism of heterotrophic bacteria. Furthermore, in these living mats, the greenish area corresponding to the presence of cyanobacteria contains a substantial reduction in the amount of carbonate mineralization that tends to disappear close to the mat/environment interface [35]. Therefore, the absence of heterotroph microorganisms and traces of mineralized sheaths in this uppermost part of the living mats rules out biologically induced mineralization. The dried crusts have been developed in a former pond of the Maquinchao Riverbed. The desiccation of the area results from a combination of increasing evaporation, lack of meteoric precipitation and absence of groundwater inputs, since the reduction of rainfall also results in groundwater depletion. Evaporation is known as an extrinsic parameter promoting carbonate precipitation [53]. Thus, we propose that the upper thin part of the dried crust may be the result of an abiotic process due to increasing the evaporation affecting the system.

In summary, the mineralization/lithification of the dried crusts is most probably the result of the heterogenous complex interplay between intrinsic and extrinsic factors that have triggered slight changes in the equilibrium during lithification. Our observations indicate that both evaporation and photosynthesis by filamentous cyanobacteria play a substantial role in mineralization. Since it is not possible to determine whether the lithified mats also include substantial SRB activity, it is difficult at this stage to assess the role of SRB in the mineralization of the calcitic matrix. However, the presence of S (Figure 4), as well as previous observations by Pacton et al. [35] in the living crust analogs, along with new DNA data, converge towards the presence and possible contribution of this group of microorganisms.

4.4. Noncarbonate Phases

There is a clear presence of Mg, Al and Si in the lithified crusts. Al-Si are usually associated with detrital phases, as shown by the higher Al content in the uppermost part of the lithified crusts (Figure 4). Enrichment in Si in certain areas of the dried crusts may be due to the presence of both detrital particles, as well as diatoms, as observed in the top part of the living crusts (Figures 4 and 6). However, the lack of clastic detrital grains in the lowest part of the crusts suggests that the Si phase is not the result of allochthonous sources but mostly from the presence of diatoms.

Certain parts of the micritic matrix are Ca-rich and associated with Si phases, whereas others are depleted in Si phases. The Al-Si and Mg-Si contents present within the carbonate matrix are mostly located in zones of dense tubular pores and/or traces of microorganisms. Pacton et al. [35] pointed

out a close connection between extracellular polymeric substances (EPS) permineralization and its further degradation and transformation into a mineralized phase associated with Mg-Si minerals. Thus, zones enriched in Ca and Si phases might be evidence for the former presence of OM (EPS or other organic compounds) and be associated with the heterotrophic degradation of OM by heterotrophic metabolisms, such as SRB, promoting carbonate precipitation. According to our observations, this Mg-Si phase is associated with both the carbonate matrix (in different proportions) and large microbial sheaths. These sheaths are enriched in Mg-Si compared to the matrix. Highly preserved sheaths display stronger signals in the silica phase (Mg and Al) relative to the Ca content (Figures 5 and 6). Hence, this suggests that the presence of a silica phase enhances the preservation of organic sheaths.

Mg-Si minerals have been reported associated with the microbial activity in different lacustrine settings (Lake Thetis and the Great Salt Lake). Their distribution has been correlated to webs of EPS [54–57] and cyanobacteria, where they have been reported in both cell walls/sheaths [50,54] and within the mineralized cells [50,58]. Diatoms are defined as possible sources of Si [35], whereas the degradation of EPS and OM in general would provide Mg [50,59]. The Mg-Si phase formation in microbialites is still poorly understood, but, nevertheless, the observed associations suggest a microbially mediated precipitation.

Thus, in the micritic calcite areas of the Maquinchao Basin crusts that are depleted in silica phases, mineralization would preferentially be triggered by extrinsic parameters (abiotic processes), whereas intrinsic parameters would have a more substantial impact on calcite precipitation in areas of micrite enriched in silica phases. Thus, the presence of a Mg-Si phase in the nodule/concretion in the lower parts of the dried crusts suggests that heterotrophic metabolism plays a role in increasing the alkalinity by degrading the OM. Conversely, the depletion in the Mg-Si phase in the calcite matrix of the uppermost part of the crust may indicate a preferential abiotic precipitation by evaporation. This is consistent with the observations of Pacton et al. [35] for the 2011 living mats, which concluded that low-Mg calcite formation was the result of OM degradation of microbial origins in the lower part of the mat.

4.5. *Introducing a Model of Formation for CaCO₃ Crusts in the Maquinchao Basin*

More extensive areas of actively accreting microbialites in modern lacustrine systems have been previously studied in South America. Although many of them have not been investigated with the detail that we present here, they might also be the result of a combination of microbial activity and extrinsic processes triggering carbonate precipitation, as we have identified in the Maquinchao millimeter-thick microbial carbonate crusts. For example, modern high-altitude lakes of Northwest Argentina contain extensive areas of active microbialite formations [15,48,49,60]. Mineralization is the result of SRB metabolic processes, whereas cyanobacteria (filaments and nonfilamentous) are the primary source of OM [15,60]. However, the resulting microstructures lack the presence of erect filaments observed in the Maquinchao Basin crusts. In fact, microbial mats mineralizing with increasing alkalinity, as a result of the heterotrophic degradation of the OM, do not display molds of erect filaments, even if an extensive content of filamentous cyanobacteria have been identified in the mats. On the other hand, filament molds are often reported in fluvial and thermal systems, where the abiotic uptake of CO₂ is the dominant parameter promoting carbonate precipitation [14,17,22,41], leading to the encrustation of the filaments. The preservation of sheaths is not reported in most of these examples. However, similar results have been reported for microbialites of Laguna Negra (Argentina) that contain preserved filaments and sheaths. In this case, the mineralization has been linked to both evaporation and microorganism activity (mostly photosynthetic activity) [48,49]. When filamentous sheaths are preserved/mineralized, mineralization is the result of CO₂ uptake by photosynthetic activity [22]. However, sheath preservation has also been observed in environments with increased alkalinity associated with extrinsic parameters, but biological processes have still had a substantial impact [17,49]. To preserve/mineralize cyanobacteria sheaths, abiotic mineralization should not completely overtake biological-induced mineralization.

Despite the relative thinness of the Maquinchao Basin crusts, mineralization does not appear to be a constant and homogenous process. The presence of erect filamentous molds, mineralized sheaths, the Mg-Si phase and the analogy with the 2011 living mats together suggest that various processes are actually involved. Paction et al. [35] concluded that the organomineralization process in the living mats was preferentially related to the microbial metabolism of heterotrophic bacteria, such as SRB. Based on the close similarities between the dried crusts and the 2011 living mats, we propose that the heterotrophic degradation of the OM has a substantial role in the crust lithification. This is further supported by the presence of a Mg-Si phase. Sheath mineralization suggests impregnation processes and a substantial impact of metabolic activity by microorganisms. Conversely, the uppermost part of the crusts and molds without sheaths suggest an increasing abiotic impact in the mineralization process. Furthermore, differences in Ca and Mg-Si enrichments have been measured in different zones of the dried crust where S is also present. The increasing incorporation of S into calcite is related to the incremental increase of this element in the pore waters due to evaporation. Therefore, extrinsic parameters and, most probably, evaporation play substantial roles in the lithification of the dried crusts, even if they have been lithified only a few years ago.

Determining precisely the individual processes leading to the mineralization of the Maquinchao Basin crusts is very complex. Dupraz et al. [24] previously noted that the mineralization of microbial mats is strongly dependent on the light balance between extrinsic and intrinsic parameters and that disentangling them is a complex and challenging matter. Our observations corroborate this statement. Our study indicates that a biologically induced mineralization process related to photosynthetic activity was combined with a subsequent enhancement of mineralization by evaporation to form the lithified carbonate crusts (Figure 8). EPS degradation has most probably triggered further mineralization by heterotrophic microorganisms. Thus, under humid conditions, mineral precipitation in the Maquinchao microbial mats is related with the heterotrophic metabolism in the lower part of the mat and photosynthetic activity in the upper part (phase 1 of Figure 8). As water levels drop, mineralization would be triggered by further metabolic processes of the microorganisms present in the mat together with abiotic processes as result of evaporation (phase 2 of Figure 8). As desiccation increases, evaporation would promote the abiotic formation of carbonate in the upper part of the microbial mat at the mat/environment interface. This could inhibit cyanobacteria photosynthesis and, conversely, promote the OM degradation by anoxygenic heterotrophs, such as SRB, thus leading to the further precipitation of calcite in the upper part of the mat (phase 3 of Figure 8). These different steps would have led to the formation of a fully mineralized crust (phase 4 of Figure 8) [61].

The 2011 living microbial mats have been previously proposed as modern analogs for the fossil microbialites present in the Maquinchao Basin [35]. Our results indicate that the presence of the erect filament molds of 8–9- μm diameters in the extensive micritic matrix can be considered to be characteristics for these crusts. The fossil microbialites of the Maquinchao Basin are composed of two main microfabrics: a laminated one (microspar/sparite and micrite) and a dense micritic one composed of erect filaments molds with the same diameters as those observed in the modern crusts. The close similarities between the 2011 living microbial mats, the microfabric of the recently formed crusts and the micritic filamentous microfabric of the Pleistocene carbonate buildups strongly support the application of the proposed analogy among these three deposits at different temporal scales. Hence, recognizing the impact of the extrinsic (evaporation) and intrinsic (photosynthesis and OM degradation by heterotrophs) in modern mineralized crust formations provides valuable criteria to identify the processes involved in the formation of micritic microfabrics in their fossil counterparts. Furthermore, these data can be further used to reconstruct the evolution of the prevailing paleoenvironmental conditions during the formation of fossil microbial buildups in many lacustrine basins.

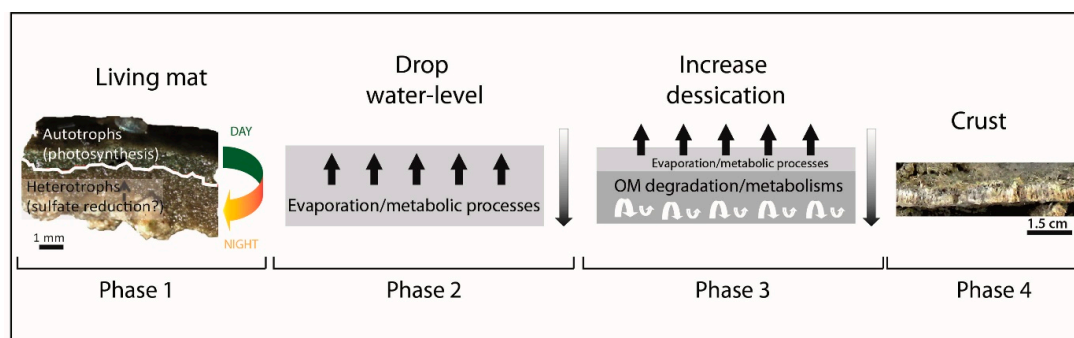


Figure 8. Proposed model of formation for the dry crust. Phase 1: Living mats are not fully layered but composed of several microorganisms, including cyanobacteria and heterotrophic microorganisms (Pacton et al., [35]). Photosynthesis is dominant during the day, whereas heterotrophic organisms, such as SRB, take over at night. Mineralization occurs mainly in the lower part of the mat and results most probably from OM degradation by heterotrophic activity [35]. Phase 2: A subsequent decrease in water level leads to evaporation, thus promoting calcium carbonate precipitation abiotically, which is further combined with carbonate produced as a result of microbial metabolic processes. Phase 3: The upper part of the mat/environment interface would eventually be completely mineralized, forming an isolating layer, thus promoting OM degradation in the lower part. Phase 4: The final product is a fully lithified carbonate crust.

5. Conclusions

The modern mineralized crusts of the Maquinchao Basin provide a unique opportunity to directly link modern mineralizing mats to fossil microbialites. The recently formed crusts (2011–2015) mainly preserved their dominant phototrophic oxygenic microbial communities as molds and/or mineralized sheaths. By comparing these crusts with their living counterparts, we can conclude that organomineralization is most probably induced by metabolic processes of former microbial communities, including oxygenic phototrophs and heterotrophs, such as SRB, and EPS degradation. Additionally, evaporation has been a dominant extrinsic parameter during the crustal formation. Thus, the similarities in the microstructures of both the recently mineralized crusts and the micritic microfacies of the Pleistocene buildups indicate that the proposed mineralization model for the modern crusts can be applied to at least some of the fossil buildups. Furthermore, this formation model developed for the Maquinchao Basin carbonate crusts can be applied to comparable fluvio-lacustrine systems of different ages in the geological record.

Author Contributions: Conceptualization, I.E., and D.A.; methodology, I.E. and D.A.; validation, M.d.P.A., A.B., C.V. and D.A.; formal analysis, I.E.; investigation, I.E.; resources, I.E., M.d.P.A. and A.B.; data curation, I.E.; writing—original draft preparation, I.E.; writing—review and editing, I.E., M.d.P.A., A.B., C.V. and D.A.; visualization, C.V. and D.A.; supervision, C.V. and D.A.; project administration, D.A. and funding acquisition, D.A. All authors have read and agreed to the published version of the manuscript.

Funding: This research was funded by the Swiss National Science Foundation, grant numbers 200021_155927 and 200021_155927/2.

Acknowledgments: We thank Rodrigo Feo for assistance during the field in windy Patagonia and Agathe Martignier for her valuable support with SEM. François Gischig is also acknowledged for technical assistance and thin-section preparations. Additionally, we kindly acknowledge the comments and suggestions of J. A. McKenzie (ETH-Zürich) and two anonymous reviewers that helped improve the final version of the manuscript.

Conflicts of Interest: The authors declare no conflicts of interest. The funders had no role in the design of the study; in the collection, analyses or interpretation of data; in the writing of the manuscript or in the decision to publish the results.

References

1. Van Gernerden, H. Microbial mats: A joint venture. *Mar. Geol.* **1993**, *113*, 3–25. [[CrossRef](#)]

2. Jorgensen, B.B.; Revsbech, N.P.; Cohen, Y. Photosynthesis and structure of benthic microbial mats: Microelectrode and SEM studies of four cyanobacterial communities. *Limnol. Oceanogr.* **1983**, *28*, 1075–1093. [[CrossRef](#)]
3. Stolz, J.F. Structure of Microbial Mats and Biofilms. In *Microbial Sediments*; Riding, R.E., Awramik, S.M., Eds.; Springer: Berlin/Heidelberg, Germany, 2000; pp. 1–8. ISBN 978-3-662-04036-2.
4. Ginsburg, R.N. Controversies about stromatolites: Vices and virtues. In *Controversies in Modern Geology*; Müller, D.W., McKENZIE, J.A., Weissert, H.J., Eds.; Academic Press: London, UK, 1991; pp. 25–36.
5. Riding, R. Microbialites, Stromatolites, and Thrombolites. In *Encyclopedia of Geobiology*; Reitner, J., Thiel, V., Eds.; Encyclopedia of Earth Sciences Series; Springer: Dordrecht, The Netherlands, 2011; pp. 635–654.
6. Burne, R.V.; Moore, L.S. Microbialites: Organosedimentary Deposits of Benthic Microbial Communities. *PALAIOS* **1987**, *2*, 241. [[CrossRef](#)]
7. Allwood, A.C.; Walter, M.R.; Kamber, B.S.; Marshall, C.P.; Burch, I.W. Stromatolite reef from the Early Archaean era of Australia. *Nature* **2006**, *441*, 714–718. [[CrossRef](#)] [[PubMed](#)]
8. Awramik, S.M.; Buchheim, H.P. A giant, Late Archaean lake system: The Meentheena Member (Tumbiana Formation; Fortescue Group), Western Australia. *Precambrian Res.* **2009**, *174*, 215–240. [[CrossRef](#)]
9. Lepot, K.; Benzerara, K.; Brown, G.E., Jr.; Philippot, P. Microbially influenced formation of 2724-million-year-old stromatolites. *Nat. Geosci.* **2008**, *1*, 118. [[CrossRef](#)]
10. Andres, M.S.; Sumner, D.Y.; Reid, R.P.; Swart, P.K. Isotopic fingerprints of microbial respiration in aragonite from Bahamian stromatolites. *Geology* **2006**, *34*, 973–976. [[CrossRef](#)]
11. Jahnert, R.J.; Collins, L.B. Characteristics, distribution and morphogenesis of subtidal microbial systems in Shark Bay, Australia. *Mar. Geol.* **2012**, *303–306*, 115–136. [[CrossRef](#)]
12. Jahnert, R.J.; Collins, L.B. Controls on microbial activity and tidal flat evolution in Shark Bay, Western Australia. *Sedimentology* **2013**, *60*, 1071–1099. [[CrossRef](#)]
13. Reid, R.P.; Macintyre, I.G.; Browne, K.M.; Steneck, R.S.; Miller, T. Modern marine stromatolites in the Exuma Cays, Bahamas: Uncommonly common. *Facies* **1995**, *33*, 1–17. [[CrossRef](#)]
14. Arp, G.; Thiel, V.; Reimer, A.; Michaelis, W.; Reitner, J. Biofilm exopolymers control microbialite formation at thermal springs discharging into the alkaline Pyramid Lake, Nevada, USA. *Sediment. Geol.* **1999**, *126*, 159–176. [[CrossRef](#)]
15. Fariás, M.E.; Rascovan, N.; Toneatti, D.M.; Albarracín, V.H.; Flores, M.R.; Poiré, D.G.; Collavino, M.M.; Aguilar, O.M.; Vazquez, M.P.; Polerecky, L. The Discovery of Stromatolites Developing at 3570 m above Sea Level in a High-Altitude Volcanic Lake Socompa, Argentinean Andes. *PLoS ONE* **2013**, *8*, e53497. [[CrossRef](#)] [[PubMed](#)]
16. Petryshyn, V.A.; Juarez Rivera, M.; Agić, H.; Frantz, C.M.; Corsetti, F.A.; Tripathi, A.E. Stromatolites in Walker Lake (Nevada, Great Basin, USA) record climate and lake level changes ~35,000 years ago. *Palaeogeogr. Palaeoclimatol. Palaeoecol.* **2016**, *451*, 140–151. [[CrossRef](#)]
17. Roche, A.; Vennin, E.; Bundeleva, I.; Bouton, A.; Payandi-Rolland, D.; Amiotte-Suchet, P.; Gaucher, E.C.; Courvoisier, H.; Visscher, P.T. The Role of the Substrate on the Mineralization Potential of Microbial Mats in a Modern Freshwater River (Paris Basin, France). *Minerals* **2019**, *9*, 359. [[CrossRef](#)]
18. Suosaari, E.P.; Reid, R.P.; Playford, P.E.; Foster, J.S.; Stolz, J.F.; Casaburi, G.; Hagan, P.D.; Chirayath, V.; Macintyre, I.G.; Planavsky, N.J.; et al. New multi-scale perspectives on the stromatolites of Shark Bay, Western Australia. *Sci. Rep.* **2016**, *6*, srep20557. [[CrossRef](#)]
19. Vasconcelos, C.; Warthmann, R.; McKenzie, J.A.; Visscher, P.T.; Bittermann, A.G.; van Lith, Y. Lithifying microbial mats in Lagoa Vermelha, Brazil: Modern Precambrian relics? *Sediment. Geol.* **2006**, *185*, 175–183. [[CrossRef](#)]
20. Arenas, C.; Jones, B. Temporal and environmental significance of microbial lamination: Insights from Recent fluvial stromatolites in the River Piedra, Spain. *Sedimentology* **2017**, *64*, 1597–1629. [[CrossRef](#)]
21. Bouton, A.; Vennin, E.; Bouille, J.; Pace, A.; Bourillot, R.; Thomazo, C.; Brayard, A.; Désaubliaux, G.; Goslar, T.; Yokoyama, Y.; et al. Linking the distribution of microbial deposits from the Great Salt Lake (Utah, USA) to tectonic and climatic processes. *Biogeosciences* **2016**, *13*, 5511–5526. [[CrossRef](#)]
22. Merz-Preiß, M. Calcification in Cyanobacteria. In *Microbial Sediments*; Riding, R.E., Awramik, S.M., Eds.; Springer: Berlin/Heidelberg, Germany, 2000; pp. 50–56; ISBN 978-3-662-04036-2.

23. Solari, M.A.; Hervé, F.; Le Roux, J.P.; Airo, A.; Sial, A.N. Paleoclimatic significance of lacustrine microbialites: A stable isotope case study of two lakes at Torres del Paine, southern Chile. *Palaeogeogr. Palaeoclimatol. Palaeoecol.* **2010**, *297*, 70–82. [[CrossRef](#)]
24. Dupraz, C.; Reid, R.P.; Braissant, O.; Decho, A.W.; Norman, R.S.; Visscher, P.T. Processes of carbonate precipitation in modern microbial mats. *Earth Sci. Rev.* **2009**, *96*, 141–162. [[CrossRef](#)]
25. Trichet, J.; Défarge, C. Non-biologically supported organomineralization. *Bull. l'Inst. Océanographique (Monaco)* **1995**, *14*, 203–236.
26. Reitner, J.; Gautret, P.; Martin, F.; Neuweiler, F. Automicrocrites in modern marine microbialite. Formation model via organic matrices (Lizard Island, Great Barrier Reef, Australia). *Bull. l'Inst. Océanographique (Monaco)* **1995**, *numéro special 14*, 237–264.
27. Altermann, W.; Böhmer, C.; Gitter, F.; Heimann, F.; Heller, I.; Lächli, B.; Putz, C. Defining biominerals and organominerals: Direct and indirect indicators of life. Perry et al., *Sedimentary Geology*, 201, 157–179. *Sediment. Geol.* **2009**, *213*, 150–151. [[CrossRef](#)]
28. Défarge, C.; Gautret, P.; Reitner, J.; Trichet, J. Defining organominerals: Comment on 'Defining biominerals and organominerals: Direct and indirect indicators of life' by Perry et al. (2007, *Sedimentary Geology*, 201, 157–179). *Sediment. Geol.* **2009**, *213*, 152–155. [[CrossRef](#)]
29. Grotzinger, J.P.; Knoll, A.H. Stromatolites in Precambrian carbonates: Evolutionary Mileposts or Environmental Dipsticks? *Annu. Rev. Earth Planet. Sci.* **1999**, *27*, 313–358. [[CrossRef](#)] [[PubMed](#)]
30. Visscher, P.T.; Reid, R.P.; Bebout, B.M.; Hoefft, S.E.; Thompson, A.T., Jr. Formation of lithified micritic laminae in modern marine stromatolites (Bahamas): The role of sulfur cycling. *Am. Mineral.* **1998**, *83*, 1482–1493. [[CrossRef](#)]
31. Pentecost, A. *Travertine*; Springer: Dordrecht, The Netherlands, 2005; ISBN 978-1-4020-3523-4.
32. Della Porta, G.D. Carbonate build-ups in lacustrine, hydrothermal and fluvial settings: Comparing depositional geometry, fabric types and geochemical signature. *Geol. Soc. Lond. Spec. Publ.* **2015**, *418*, SP418.4. [[CrossRef](#)]
33. Visscher, P.T.; Stolz, J.F. Microbial mats as bioreactors: Populations, processes, and products. *Palaeogeogr. Palaeoclimatol. Palaeoecol.* **2005**, *219*, 87–100. [[CrossRef](#)]
34. Eymard, I.; Bilmes, A.; Alvarez, M.D.P.; Feo, R.; Hunger, G.; Vasconcelos, C.; Ariztegui, D. Growth morphologies and plausible stressors ruling the formation of Late Pleistocene lacustrine carbonate buildups in the Maquinchao Basin (Argentina). *Depos. Rec.* **2019**, *5*, 498–514. [[CrossRef](#)]
35. Pacton, M.; Hunger, G.; Martinuzzi, V.; Cusminsky, G.; Burdin, B.; Barmettler, K.; Vasconcelos, C.; Ariztegui, D. Organomineralization processes in freshwater stromatolites: A living example from eastern Patagonia. *Depos. Rec.* **2015**, *1*, 130–146. [[CrossRef](#)]
36. Bilmes, A.; D'Elia, L.; Lopez, L.; Richiano, S.; Varela, A.; del Pilar Alvarez, M.; Bucher, J.; Eymard, I.; Muravchik, M.; Franzese, J.; et al. Digital outcrop modelling using “structure-from-motion” photogrammetry: Acquisition strategies, validation and interpretations to different sedimentary environments. *J. S. Am. Earth Sci.* **2019**, *96*, 102325. [[CrossRef](#)]
37. Visscher, P.T.; Reid, R.P.; Bebout, B.M. Microscale observations of sulfate reduction: Correlation of microbial activity with lithified micritic laminae in modern marine stromatolites. *Geology* **2000**, *28*, 919–922. [[CrossRef](#)]
38. Bathurst, R.G.C. Boring algae, micrite envelopes and lithification of molluscan biosparites. *Geol. J.* **1966**, *5*, 15–32. [[CrossRef](#)]
39. Payandi-Rolland, D.; Roche, A.; Vennin, E.; Visscher, P.T.; Amiotte-Suchet, P.; Thomas, C.; Bundeleva, I.A. Carbonate Precipitation in Mixed Cyanobacterial Biofilms Forming Freshwater Microbial Tufa. *Minerals* **2019**, *9*, 409. [[CrossRef](#)]
40. Freytet, P.; Verrecchia, E.P. Freshwater organisms that build stromatolites: A synopsis of biocrystallization by prokaryotic and eukaryotic algae. *Sedimentology* **1998**, *45*, 535–563. [[CrossRef](#)]
41. Gradziński, M. Factors controlling growth of modern tufa: Results of a field experiment. *Geol. Soc. Lond. Spec. Publ.* **2010**, *336*, 143–191. [[CrossRef](#)]
42. Pedley, M. Freshwater (phytoherm) reefs: The role of biofilms and their bearing on marine reef cementation. *Sediment. Geol.* **1992**, *79*, 255–274. [[CrossRef](#)]
43. Pedley, M. Ambient Temperature Freshwater Microbial Tufas. In *Microbial Sediments*; Riding, R.E., Awramik, S.M., Eds.; Springer: Berlin/Heidelberg, Germany, 2000; pp. 179–186. ISBN 978-3-662-04036-2.
44. Pedley, H.M. Classification and environmental models of cool freshwater tufas. *Sediment. Geol.* **1990**, *68*, 143–154. [[CrossRef](#)]

45. Barbin, V.; Schvoerer, M. Cathodoluminescence géosciences. *Comptes Rendus de l'Académie des Sci. Ser. IIA Earth Planet. Sci.* **1997**, *325*, 157–169. [[CrossRef](#)]
46. Machel, H.G. Application of Cathodoluminescence to Carbonate Diagenesis. In *Cathodoluminescence in Geosciences*; Pagel, M., Barbin, V., Blanc, P., Ohnenstetter, D., Eds.; Springer: Berlin/Heidelberg, Germany, 2000; pp. 271–301. ISBN 978-3-662-04086-7.
47. Merz-Preiß, M.; Riding, R. Cyanobacterial tufa calcification in two freshwater streams: Ambient environment, chemical thresholds and biological processes. *Sediment. Geol.* **1999**, *126*, 103–124. [[CrossRef](#)]
48. Gomez, F.J.; Mlewski, C.; Boidi, F.J.; Fariás, M.E.; Gérard, E. Calcium Carbonate Precipitation in Diatom-rich Microbial Mats: The Laguna Negra Hypersaline Lake, Catamarca, Argentina. *J. Sediment. Res.* **2018**, *88*, 727–742. [[CrossRef](#)]
49. Gomez, F.J.; Kah, L.C.; Bartley, J.K.; Astini, R.A. Microbialites in a High-Altitude Andean Lake: Multiple Controls on Carbonate Precipitation and Lamina Accretion. *PALAIOS* **2014**, *29*, 233–249. [[CrossRef](#)]
50. Wacey, D.; Urosevic, L.; Saunders, M.; George, A.D. Mineralisation of filamentous cyanobacteria in Lake Thetis stromatolites, Western Australia. *Geobiology* **2018**, *16*, 203–215. [[CrossRef](#)] [[PubMed](#)]
51. Dupraz, C.; Visscher, P.T. Microbial lithification in marine stromatolites and hypersaline mats. *Trends Microbiol.* **2005**, *13*, 429–438. [[CrossRef](#)]
52. Vasconcelos, C.; Dittrich, M.; McKenzie, J.A. Evidence of microbiocoenosis in the formation of laminae in modern stromatolites. *Facies* **2014**, *60*, 3–13. [[CrossRef](#)]
53. Mattson, M.D. Alkalinity of Freshwater. In *Reference Module in Earth Systems and Environmental Sciences*; Elsevier: Amsterdam, The Netherlands, 2014; ISBN 978-0-12-409548-9.
54. Burne, R.V.; Moore, L.S.; Christy, A.G.; Troitzsch, U.; King, P.L.; Carnerup, A.M.; Hamilton, P.J. Stevensite in the modern thrombolites of Lake Clifton, Western Australia: A missing link in microbialite mineralization? *Geology* **2014**, *42*, 575–578. [[CrossRef](#)]
55. Pace, A.; Bourillot, R.; Bouton, A.; Vennin, E.; Galaup, S.; Bundeleva, I.; Patrier, P.; Dupraz, C.; Thomazo, C.; Sansjofre, P.; et al. Microbial and diagenetic steps leading to the mineralisation of Great Salt Lake microbialites. *Sci. Rep.* **2016**, *6*, 31495. [[CrossRef](#)]
56. Wacey, D.; Gleeson, D.; Kilburn, M.R. Microbialite taphonomy and biogenicity: New insights from NanoSIMS. *Geobiology* **2010**, *8*, 403–416. [[CrossRef](#)]
57. Bontognali, T.R.R.; Vasconcelos, C.; Warthmann, R.J.; Bernasconi, S.M.; Dupraz, C.; Strohmenger, C.J.; McKenzie, J.A. Dolomite formation within microbial mats in the coastal sabkha of Abu Dhabi (United Arab Emirates). *Sedimentology* **2010**, *57*, 824–844. [[CrossRef](#)]
58. Zeyen, N.; Benzerara, K.; Li, J.; Groleau, A.; Balan, E.; Robert, J.-L.; Estève, I.; Tavera, R.; Moreira, D.; López-García, P. Formation of low-T hydrated silicates in modern microbialites from Mexico and implications for microbial fossilization. *Front. Earth Sci.* **2015**, *3*. [[CrossRef](#)]
59. Souza-Egipsy, V.; Wierzchos, J.; Ascaso, C.; Nealson, K.H. Mg–silica precipitation in fossilization mechanisms of sand tufa endolithic microbial community, Mono Lake (California). *Chem. Geol.* **2005**, *217*, 77–87. [[CrossRef](#)]
60. Fariás, M.E.; Poiré, D.G.; Arrouy, M.J.; Albarracin, V.H. Modern Stromatolite Ecosystems at Alkaline and Hypersaline High-Altitude Lakes in the Argentinean Puna. In *STROMATOLITES: Interaction of Microbes with Sediments*; Tewari, V., Seckbach, J., Eds.; Cellular Origin, Life in Extreme Habitats and Astrobiology; Springer: Dordrecht, The Netherlands, 2011; pp. 427–441. ISBN 978-94-007-0397-1.
61. Bruggmann, S. Growth Constraints and Environmental Influences on a Modern Stromatolite, Lagoa Vermelha, Brasil. Master's Thesis, ETH-Zürich, Zürich, Switzerland, 2015.

